

System Engineering, Design, Integration, and Qualification of Electric Propulsion Space Experiment

Mary M. Kriebel*

TRW, Redondo Beach, California 90278

Electric arcjet propulsion systems provide an attractive option for enhancing spacecraft payload mass, increasing on-orbit lifetimes, and reducing launch costs as long as the mission can accommodate the low-thrust levels inherent to electric propulsion. To demonstrate this technology, a 30-kW class ammonia arcjet flight experiment was designed, built, qualified, and operated in space as part of the 30-kW Class Arcjet Advanced Technology Transition Demonstration Program. The engineering qualification and spacecraft integration of the propulsion system are summarized.

Introduction

BEFORE 1990, over 75 spacecraft were flown using electric propulsion (EP) for attitude control or orbit adjustments and over 10 experimental spacecraft were flown to perform EP thruster demonstrations or spacecraft interface characterization. Of these spacecraft, the highest powered EP device was operated at 3 kW (Ref. 1). However, there was still considerable concern regarding the integration of EP thrusters onto spacecraft due to plume impacts such as thermal loading on spacecraft surfaces, interference with spacecraft communication, and contamination of critical surfaces (solar arrays, thermal radiators, etc.). Hence, a considerable amount of government- and commercial industry-sponsored testing was performed in ground-based laboratories to address the integration concerns.^{2,3} Again, most of these efforts were concentrated on low-power (<2.2-kW) arcjet thrusters. These thrusters would ultimately see widespread use by the turn of the century as a result of these efforts.⁴ However, there is one effort, the Arcjet Advanced Technology Transition Demonstration (Arcjet ATTD) Program, that stands out. The objective of this program was to develop, demonstrate, and flight qualify a high-power (>26-kW) arcjet propulsion unit that would measure plume deposition, electromagnetic interference, thermal radiation, and arcjet-induced acceleration in space. These measurements were chosen to address the specific operational issues listed, but for a much higher power class of EP thruster.

The flight unit, shown schematically in Ref. 5, consisted of a low-impedance 26-kW arcjet, power conditioning unit (PCU), propellant feed subsystem (PFS), command/control subsystem (CCS), diagnostic package, power subsystem (PSS), thermal management subsystem (TMS), and the integrating structure. Figure 1 shows the actual flight unit prior to protoflight testing. TRW Space and Technology Division was responsible for the system engineering, the mechanical, electrical, and thermal integration engineering, and the design and development of the diagnostic package. Primex Aerospace Company (PAC) designed, developed, and fabricated the arcjet, PCU and PFS, and Space Power, Inc., provided input to the PCU design. Orbital Sciences Corporation was responsible for the CCS, structure, and integration of the flight unit. TRW completed the hardware development effort by performing the qualification test-

ing of the flight unit. The Air Force Research Laboratory (AFRL) was responsible for integration of the delivered flight experiment, renamed Electric Propulsion Space Experiment (ESEX), onto the Advanced Research and Global Observation Satellite (ARGOS) and ESEX flight operations.

Like many experimental and demonstration spacecraft, the budget available for such an endeavor was limited. Hence, the program success was dependent on the use of 1) existing arcjet, PCU, and PFS technology as the basis for the flight hardware; 2) existing space-qualified instruments for the arcjet flight unit diagnostic package; 3) space-qualified design approaches for the remaining flight unit support hardware; and 4) the protoflight approach to flight unit qualification.

Approach

The flight unit development, demonstration, and flight qualification was performed in three phases: phase I, system design; phase II, development test vehicle buildup, test, and integration; and phase III, flight qualification and delivery. During phase I, the engineering design of all subsystems and the flight unit was performed. Preliminary developmental testing was also performed using a government-furnished arcjet and a breadboard PCU to establish detailed technical criteria regarding the startup of the arcjet with the PCU. Phase I was concluded with the presentation of the preliminary flight unit design to AFRL at the preliminary design review (PDR) in July 1991.

During phase II, fabrication and testing of development hardware was conducted and detailed design changes were incorporated based on these test results. Figures 2 and 3 show the details of the program flow during phase II between PDR and flight-qualification testing. This program plan was developed to address key issues, for example, arcjet and PCU development, early in phase II while addressing system design and interfaces later in phase II pending identification of the host vehicle. The final flight design was presented to AFRL at the program critical design review (CDR) in December 1993. Following AFRL's approval of the CDR design, some engineering model (EM) hardware was refurbished for flight (Fig. 3). The flight PFS, a flight arcjet, and a flight PCU were fabricated and assembled from all new components.

Phase III of the program began at the completion of flight unit assembly and initial functional testing. During this phase, the flight unit was protoflight-qualification tested utilizing an arcjet simulator as required. This testing consisted of flight software verification, thermal vacuum, random vibration, electromagnetic compatibility (EMC), proof pressure and leak testing of the propulsion subsystem, and integrated system tests. After completion of its ground qualification test, the flight unit was delivered to AFRL at the The Boeing Company in Seal Beach, California for integration onto the ARGOS spacecraft.

Received 18 January 2001; revision received 13 February 2002; accepted for publication 1 March 2002. Copyright © 2002 by the American Institute of Aeronautics and Astronautics, Inc. All rights reserved. Copies of this paper may be made for personal or internal use, on condition that the copier pay the \$10.00 per-copy fee to the Copyright Clearance Center, Inc., 222 Rosewood Drive, Danvers, MA 01923; include the code 0748-4658/02 \$10.00 in correspondence with the CCC.

*Propulsion Systems Manager, Lasers, Sensors and Propulsion Products, Engineering Division, M/S 140/2108, One Space Park. Senior Member AIAA.

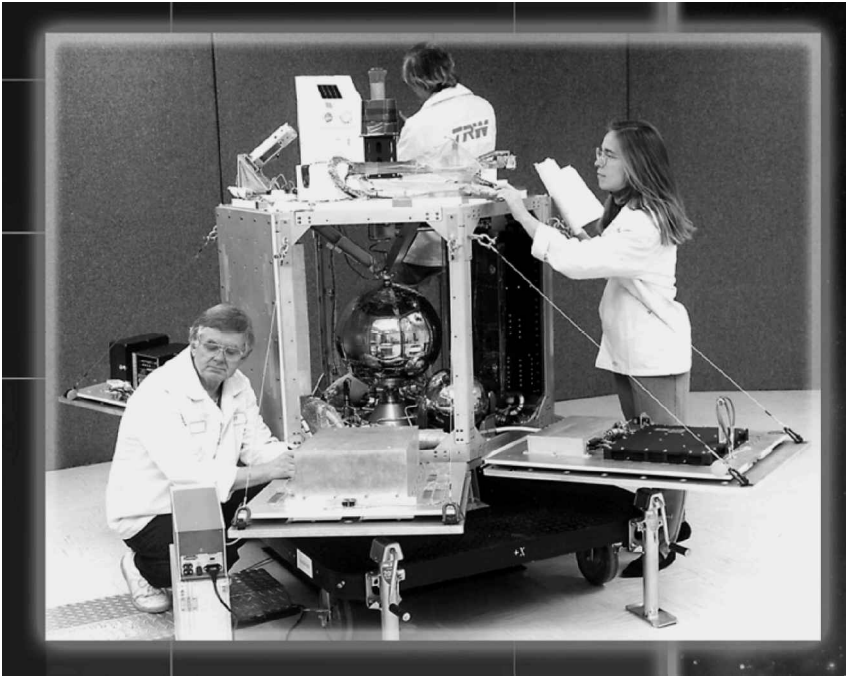


Fig. 1 Arcjet ATTD flight unit.

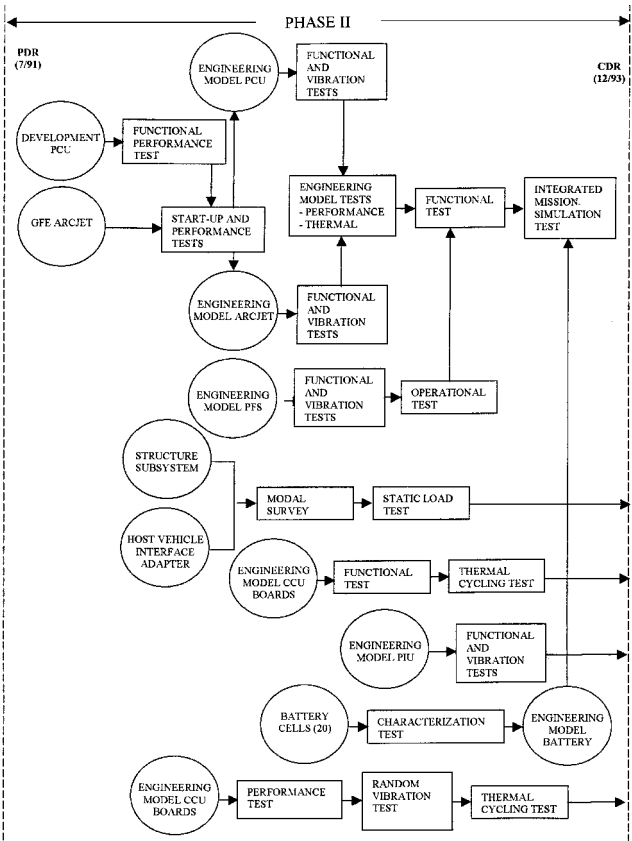


Fig. 2 Arcjet ATTD phase II program plan (PDR to CDR).

Phase I: Design

The following paragraphs describe the work that was performed from the start of the program in February 1990 until the PDR, which was held in July 1991.

System Design

The primary system-level activity of this phase was the generation and continuous refinement of the system and subsystem-level design requirements. At the start of phase I, a system requirements review

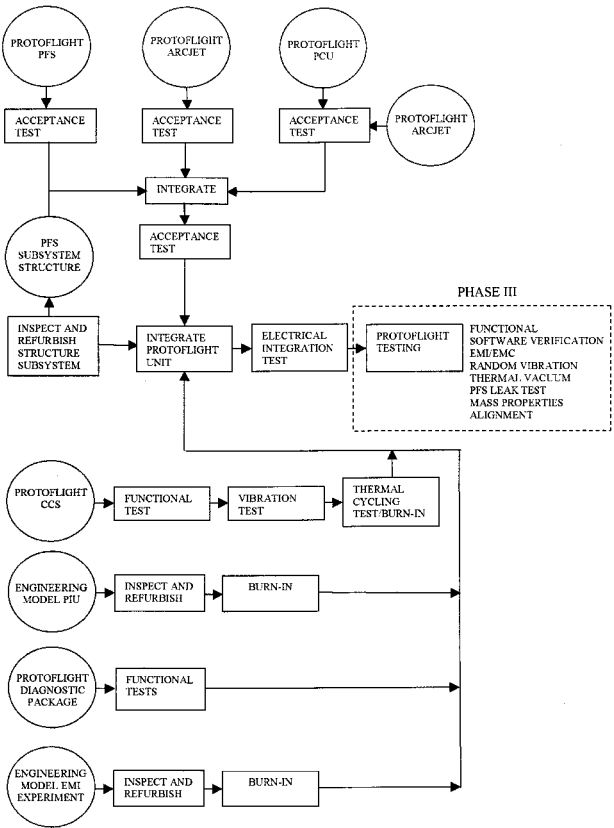


Fig. 3 Arcjet ATTD phase II (post-CDR) and phase III program plan.

(SRR) was conducted to establish top level and derived requirements at the system and subsystem levels. These key requirements are shown in Table 1.

The initial physical design was driven by the requirement that the flight unit be compatible with the Pegasus™ launch vehicle, but remain flexible enough to meet many other launch vehicle launch environments. This was because the launch vehicle had not been identified at initiation of the contract. Therefore, the flight unit was designed to fit within the payload envelope of the Pegasus fairing,

and the weight was controlled within its launch capability. At SRR, this weight was allocated as shown in Table 2. Ultimately, the weight of the flight unit increased due to design maturity and as a result of weight vs cost trades. In phase II, the increased launch capability of the ARGOS Delta II launch vehicle was taken advantage of for simpler, less costly design approaches.

As can be noted from Table 1, no specific power requirement was levied on ESEX with the exception of the operating power of the arcjet. Because a system power requirement was not designated until phase II with the assignment of ESEX to ARGOS, the power required for the flight unit auxiliary functions was simply tracked during phase I.

The high current used by the Arcjet ATTD flight unit required a conservative grounding philosophy. The requirements imposed on the grounding scheme were high-power ground at the anode, low-power ground for the 28-V dc bus at the power integration unit (PIU) and distributed signal grounds and isolated power for diagnostics and the command/control unit (CCU). This grounding philosophy also featured no power current flow through the structure. The grounding scheme for the interface was the host vehicle was grounded at the host vehicle power system and isolated power was sent to the PIU.

Table 1 Arcjet ATTD program requirements

Specification	Requirement
System definition	Flight unit shall consist of an arcjet, PCU, CCS, PFS, diagnostic package, power source, TMS, subsystem interfaces, and system packaging
System functions	Perform of all diagnostic sensors, start arcjet propulsion system, monitor all operations, detect any malfunctions, shut down the system, and perform restarts as required
Arcjet electrical input Power	Nominal operating power: 26 kW
Design life	1500 h and 400 on/off cycles
Numbers of firings	Not less than 10, 15 min firings
Time between firings	Not more than 100 h
Specific impulse	Not less than 800 ± 20 s
Thrust	Approximately 2 N (vacuum)
Lifetime	Not less than 1000 h
Power source	Bank of batteries capable of recharge within 100 h
Weight	418 kg (920 lbm)
Volumetric envelope	Maximum height: 150.5 cm (59.26 in.) maximum diameter: 125 cm (49.2 in.)
Propellant	Ammonia
Diagnostic package Instrumentation	Shall include instrumentation to measure thrust, mass flow, arcjet plume contamination of spacecraft surfaces, EMI, and temperatures. Video camera shall be included for video documentation of nozzle and plume luminescence
Testing and flight unit qualification	MIL-STD-1540B and MIL-HDBK-343 (Class C)

Arcjet and PCU Design

The program approach for the arcjet design started with the AFRL 26-kW arcjet design previously developed for AFRL.⁴ Minimal internal design changes were made to the thruster, and the geometry of the electrodes was unchanged. The phase I design work converted this laboratory model to the flight-weight, space-qualified arcjet shown in Ref. 6 and produced the power cable that supplied the high-voltage, high-current power to the arcjet from the PCU. The arcjet was required to produce greater than 800 s specific impulse I_{sp} and approximately 2 N of thrust, and the arcjet power cable had to minimize radiated emissions so as to not interfere with flight unit operations. Therefore, a triaxial cable with helical scoring for flexibility was designed and tested. The baseline PCU design incorporated a three-phase buck regulator concept. However, considerable design work was required to define accurately the startup parameters and to create a flight-qualified unit. Details of this arcjet, cable, and PCU development efforts are provided in Ref. 6.

PFS Design

The PFS, shown schematically in Fig. 4, was designed such that ammonia was stored in a spherical propellant tank, which had two polar heaters, one at the outlet of the tank and one at the opposite end. These heaters allowed preferential heating of either end of the tank to help position ammonia gas for the outflows. To assure full vaporization of the ammonia, an enhanced feedline heater (EFH) was developed for the system. The EFH was a segment of the propellant line immediately downstream of the propellant tank outlet packed with a metallic wick and heated with 300-W heaters. The vaporized ammonia was then contained in a plenum tank for subsequent feed into the arcjet. Flow was measured and controlled by an orificed manifold using output signals of two pressure transducers and one thermistor. This approach, described in more detail in

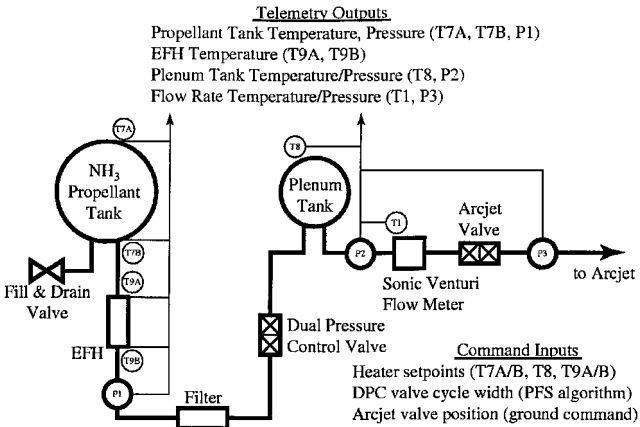


Fig. 4 Schematic of the PFS.

Table 2 Arcjet ATTD system weight summary

Subsystem or major component mass, kg	Initial mass estimate with recommended contingency, kg	Final mass allocations at CDR, kg	Cause of mass weight delta
Arcjet and power Cable	13.5	12.7	Cable design
PCU	37.5	48.2	Overall design growth
PFS	12.5	15.9	Addition of EFH and mounting structure
Diagnostic package	13.2	15.9	Increases in component weight
PSS	232.2	232.7	High-voltage protection and harness growth
Thermal management	23.7	48.2	Beryllium heat sink for PCU
Command/control	17.4	4.5	Overall design growth
Structure	39.2	69.5	Overall design growth
Subtotal	389.2	446.8	
Propellant	15.9	4.5	Reduced to reflect NH ₃ needed
Total	365.9	451.3	

Ref. 6, performed very well in providing the necessary flow accuracy required by the arcjet.

Diagnostic Package Design

The key requirements for the diagnostics package are listed in Table 3. Also provided are the specific measurements and instruments used to make the measurements. These instruments were chosen to collect information regarding arcjet performance and spacecraft interaction that cannot be adequately quantified in ground tests. To determine the optimum locations of the diagnostic package instruments, the arcjet thruster plume flowfield was analytically modeled. The analysis results helped to locate the four thermoelectric quartz crystal microbalances (TQCMs) and the solar cells and were used to determine the potential condensation from the arcjet plume. Of the primary constituents of the arcjet plume (molecular and atomic nitrogen and hydrogen and NH), only NH was expected to condense. Metallic constituents, tungsten and thorium, from the arcjet, were also expected to condense, but the total deposition during the mission was expected to be negligible.

TQCMs, solar cells, and radiometers were chosen for measuring plume contamination. TQCMs measure deposition of contaminants per unit surface of an exposed crystal. The monitor consists of a quartz crystal vibrating in shear mode that stabilizes at the resonant frequency of an oscillator. As the mass deposition on the surface increases, the beat frequency of the oscillator changes. There is a direct correlation between frequency and mass accumulation per unit surface area. These TQCMs were temperature controlled by means of a thermoelectric two-stage cooler set to a desired cold temperature for deposition measurements. The subsequent heating of the elements would ideally allow thermal gravimetric desorption of the crystals in flight. This desorption technique permits identification of the collected contaminants by measuring the temperature at which vaporization occurs. However, in practice, this proved difficult.

The diagnostic package had four TQCMs operating from a single electronics unit. This hardware package was available off the shelf. The first sensor (TQCM 4) monitored contamination in the back-flow region, where the contaminants were most likely to exist, and was located on the deployable boom to allow far-field extrapolations. The three remaining sensors were positioned to take relative plume contamination measurements. TQCMs 2 and 3 were mounted directly on top of the diagnostic package platform. TQCM 1 was mounted above the diagnostic platform at approximately the same height above the platform as the arcjet thruster exit plane next to the solar cells. This TQCM sensor was used to help determine if plume contamination occurred on the witness samples and what the condensable deposits were.

The second element of the plume contamination experiment was the solar cell deposition experiment. Eight cells were mounted at a 45-deg angle from the arcjet centerline to receive exposure to the sun, as well as the arcjet. There were two circuits of four cells in series; one circuit would measure the short circuit current, whereas the second would measure load voltage. The type of solar cell cho-

sen was gallium arsenide, which is less sensitive to the infrared frequencies expected from the arcjet. The spectral radiance of the arcjet anode is greatest in the wavelength range of 690–1200 nm, whereas solar cells respond to light in the range of 300–1200 nm. This correlation allowed direct measurement of the effect of an arcjet on a solar array. A thermistor was also mounted on the back of the baseplate to provide temperature data during flight. The cells' open-circuit voltage and closed-circuit current was monitored before arcjet operations to obtain baseline data throughout the orbit cycle. The changes in these data observed during and after arcjet operations, after correcting for temperature variations, could be viewed as possible plume deposition effects. Performing a thermal gravimetric analysis on TQCM 1 could then, potentially, provide insight into the source of the contamination on the solar cells.

The last element of the plume contamination experiment was four radiometers for measuring heat energy flux during arcjet operations. These radiometers were designed and qualified for this flight experiment. These radiometers were positioned on the diagnostic platform and on the witness plate directly viewing the arcjet body. The specific locations and the radiometer thermistor data provided the data necessary to establish the heat flux during arcjet operations as a function of position and angle.

For optical measurements, a video camera with a permanent filter to attenuate the anode glow was used to record plume luminescence. The bandwidth selected for the camera was 656-nm because PAC had previous experience with this type of filter and because the hydrogen alpha line radiates at 656 nm. The camera collected the optical image and provided the data to the CCU to process. The processing results in a color-coded temperature band in the anode to indicate whether or not hot spots developed due to arc attachment problems with the plume showing up as an intense colored area.

A laboratory video camera equivalent to the flight video camera was used during laboratory arcjet firings to determine the optimum aperture setting for the flight camera because this could not be varied on-orbit. Based on the video camera images of the arcjet plume, a baseline camera f-stop of 8.0 was chosen. For each arcjet firing, a series of frames from the camera were stored in the frame-grabber unit for transmission to the ground at a later time. Selection of when within the arcjet firing these frames were taken and at what sample rate could be varied by ground command.

For electromagnetic interference (EMI) measurements, an experiment was designed to monitor EMI in four communication frequency bands centered at 2, 4, 8, and 12 GHz. Two spiral cavity antennas were used to pick up these signals. One was mounted on the diagnostic package platform and the second was mounted at the end of the deployable boom to allow measurements in both the near- and far-field regions. The 2, 4, 8 and 12 GHz frequencies were selected based on data gathered from the Arcjet System Integration Demonstration program.³ A saturated reading was expected at 2 GHz, and a null reading was expected at 12 GHz, but these readings would help bound the EMI characteristics of the arcjet, as well as to provide credibility to those taken at 4 and 8 GHz. Because an off-the-shelf unit for collecting these data did not exist, a

Table 3 Diagnostic package instrumentation

Requirement	Capability	Verification method
Measure thruster performance		
Thrust	Accelerometer	Computed from measurement and mass
Mass Flow	Mass flow meter	Measured
Thruster voltage and current	Voltmeter, ammeter	Measured
Measure plume contamination (function of radius and angle)	TQCM	Measurements in four positions
Determine plume effects on		
Solar Arrays	Solar array witness plate	Measurements
Typical space vehicle structures		Provide flowfield for further analysis and test
Refractory metals		
Thermal radiation flux (function of radius and angle)	Radiometers	Measurements in four positions
EMI (function of radius and angle)	Radiated EMI experiment	Measurements in two positions
Document nozzle and plume luminescence	Video camera	Observation
Relate collection data to expected results at 30 m		Analysis

breadboard unit of the EMI electronics unit was designed, built, and tested during phase I.

An accelerometer was used to determine the arcjet thrust. After the spacecraft wet weight before launch and accelerations during arcjet firings were measured, the thrust of the arcjet can be calculated. The arcjet I_{sp} was then calculated from the mass flow measurements made by the PFS, combined with the calculated thrust. Additional telemetry collected for the arcjet via the PCU included arcjet input current and voltage. When the thrust, mass flow, and power data are used, the arcjet efficiency can be calculated.

PSS Design

The PSS consisted of a high-voltage silver–zinc battery and the PIU. The battery was dedicated to providing power to the PCU and arcjet and was recharged by the ARGOS solar array. The PIU was the electrical interface between ESEX and ARGOS, distributing and converting host vehicle power to the CCS, PFS, PCU, diagnostic experiment, and thermal management subsystem as well as providing telemetry conditioning.

Two prototype KilovacTM relays (600-A, make-and-break load, hermetically sealed switches) were used in the PSS to isolate the PCU from the high-voltage batteries before adequate outgassing occurred within the PCU to prevent corona discharge damage. Although these parts had not completed a formal qualification program, they were selected because no other relays were available that met the requirements. The risk of using these relays was reduced by including the flight relays in the phase II structural qualification testing because this was the best means to verify flight readiness without subjecting them to a full component qualification program. In addition, the flight requirements were also small (one cycle). Flight results confirmed the successful operation of these components.

TMS Design

Two key requirements drove the TMS design. The design was to accommodate a broad range of space missions without dependence on the host vehicle for maintaining thermal control. The TMS was also required to maintain all components within their qualified temperature limits during any phase of the experiment including a steady-state arcjet firing. This requirement was important because, at an input power of 28 kW and a PCU efficiency of at least 93%, more than 1900 W of heat were required to be removed from the PCU and radiated to space.

All electronic boxes of the flight experiment were mounted to the side panels of the flight experiment to allow internal box heat to be conducted to side panel silvered Teflon[®] tape (STT) radiators. The one exception to this was the panel on which the PCU was mounted. The heat needed to be rejected away from the PCU was greater than any amount that STT radiators alone could handle. In the initial design, the PCU was mounted to a phase change material (PCM) panel. The panel is similar to a honeycomb panel, except that it is filled with a paraffinlike material that melts as it is heated. During the latter part of phase I, the PCU panel was changed to a beryllium panel that stored the PCU heat dissipations in the combined thermal mass of the beryllium panel and the PCU. Although heavier than the PCM panel, the beryllium panel was chosen as a better technical solution and because of the significant development and fabrication cost savings. Similar to the PCU, the silver–zinc battery subassemblies stored the 1600 W generated per battery subassembly during the battery discharge (arcjet firing) and released it through STT radiator areas on the three battery panels.

Structure Design

During phase I of the Arcjet ATTD program, the launch vehicle and loads for the flight experiment were undefined. Therefore, a major portion of the structure design effort was purposely delayed until after these interfaces were established. However, there were basic requirements that could be used to develop the preliminary design. The flight experiment envelope requirement was known, and the design was required to provide modularity to allow for quick and easy replacement of major components. As a derived requirement,

the structure was to provide enough radiator area for all of the electronic components. To meet these requirements, a hexagonal body design was chosen that allowed the electronic boxes to be mounted to the six side panels and their radiators mounted on the exterior of the experiment for heat rejection to space. These side panels could be individually removed from the hexagonal structure for access to any of the components within the interior of the flight experiment. Two subsystem platforms were the top and bottom structural components. The propulsion platform provided the mounting surface for all PFS components, and the arcjet and diagnostic sensors were mounted on the diagnostic platform.

The core frame used for mounting of the platforms and panels was a stand-alone design such that it did not require either platform to integrate the side panels. This was an important integration feature allowing the flight PFS to be built at one facility while the remainder of the flight experiment was integrated at another.

Phase II: Development Test Vehicle Buildup, Test, and Integration

Phase II consisted of fabricating development hardware, conducting subsystem development and EM tests, upgrading the detailed design before fabrication of the flight hardware, and integrating the flight unit. At the beginning of phase II, the Arcjet ATTD host spacecraft was identified as the ARGOS satellite. Along with this came the identification of new requirements, interfaces, and launch environments, and the flight unit experienced design updates to comply with these changes. Because the flight unit design had been constrained in size and driven by very conservative launch environment requirements, the transition to the ARGOS spacecraft was fairly smooth.

With the host vehicle identified, a specific ESEX power profile requirement was established. Throughout phase II, this power profile saw much iteration as the requirements from ARGOS and the Arcjet ATTD flight unit design matured. The power profile evolved to the one shown in Fig. 5.

ARGOS also required ESEX to have the arcjet aligned to the ARGOS c.g. to prevent the arcjet from overwhelming the attitude control system and causing the vehicle to tumble. Therefore, an alignment requirement that stipulated radial and angular offset limits was defined by the line in Fig. 6. With the assumption that the arcjet thrust vector was coincident with the thruster centerline, it was determined that the flight unit would meet the alignment requirement with the implementation of specific design and alignment controls. Another spacecraft-level concern was the state of charge of the battery at the completion of the ESEX operation. Because other ARGOS experiments were to operate after ESEX, the battery subassemblies could not impact the other experiments. Specific concerns were electrolyte leakage and electrical shorting within the battery. The concern of electrolyte leakage was eliminated because the existing cell design included internal matting material to contain the electrolyte within the battery. However, the potential for a battery short remained. Discharging the battery to 0 V would eliminate the potential for a dead short. However, the operational plan and electrical design for ESEX did not include any provisions for a complete discharge of the battery. Therefore, each battery pack was outfitted with separate discharge circuits consisting of a thermostat and resistor circuit. The TMS and CCS systems were designed such that the resistor discharge circuit, activated after the completion of the ESEX experiment, continually discharged each battery assembly and prevented electrolyte freezing. Although this design did have some potential single-point failures, the identified risks were accepted to minimize the impact on the ARGOS system.

ESEX was one of nine experiments flown aboard ARGOS. Many of those experiments involved sensitive optical devices. Therefore, the ARGOS operational plan had ESEX perform its mission first. After ESEX completed its mission, the protective covers on these optics were deployed, and the remaining payloads commenced operations. Because of the desire to activate these experiments as quickly after launch as possible, ARGOS performed their initial on-orbit check-out in two weeks. Therefore, ESEX performed an analysis to verify the adequacy of the flight unit design to relieve the internal

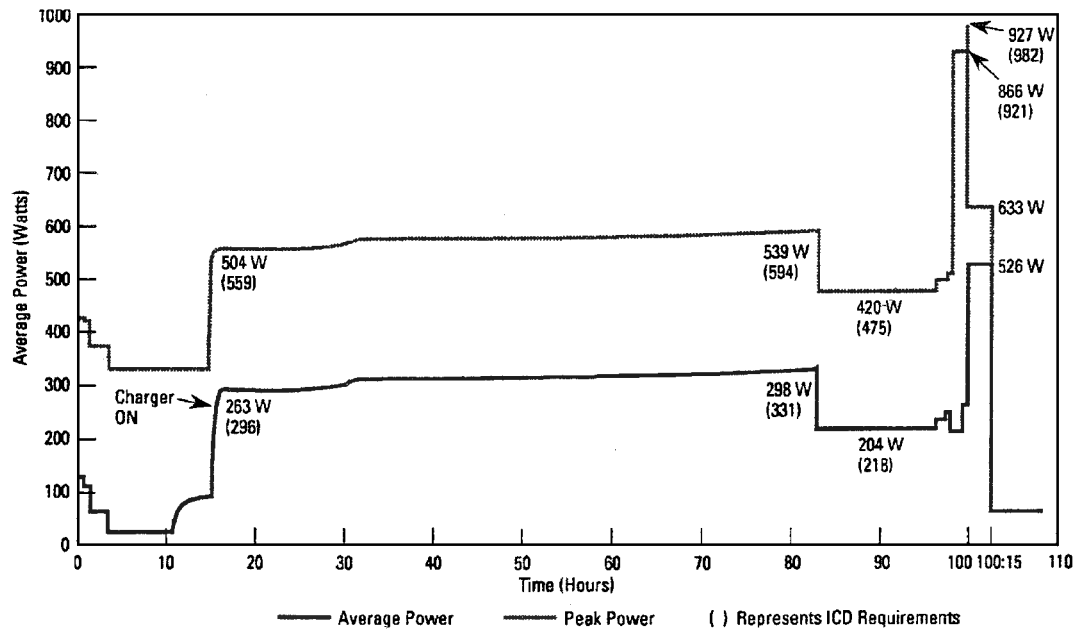


Fig. 5 Phase II power profile.

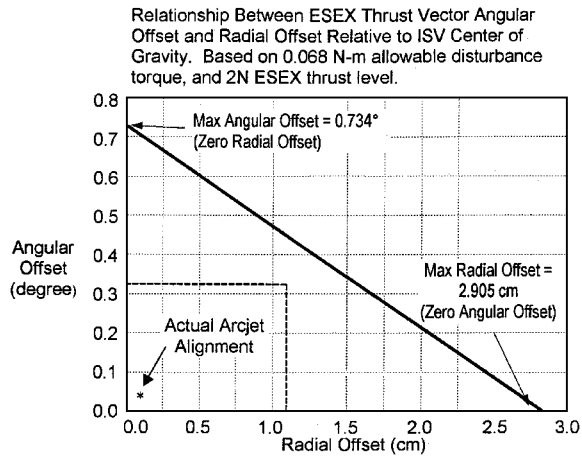


Fig. 6 Arcjet ATTD alignment requirement and capability.

pressure at the conclusion of the on-orbit checkout to below the critical pressure of 1×10^{-3} torr (specified as the upper limit permitted for powering up the high-voltage circuitry within the PCU). The total outgassing mass flow rate was computed based on materials, areas, and temperatures along with the available data on the outgassing rates of the materials. It was conservatively estimated that, at the end of the two weeks on-orbit, the pressure within the flight unit would be 4×10^{-5} torr, a factor of 25 below the critical pressure.

After being assigned as a payload aboard the ARGOS spacecraft, the diagnostic package design was reviewed, and the locations of instrumentation were definitized. The primary design constraints for locating the instruments were 1) maximize the exposure of the solar cells to sunlight, 2) deploy EMI antenna boom into the Y plane to avoid interference with the reaction control thrusters of the ARGOS spacecraft, and 3) minimize EMI cable lengths to minimize losses within the cables. All instruments were located as shown in Fig. 7.

A key test performed during phase II was the integrated mission simulation (IMS) test. This test integrated many components of the flight unit together to verify they would operate compatibly and to identify any interactions between them. Although the original intent was to test only the performance of the EM arcjet, PCU, PFS, and battery together, several diagnostics were added. Added to this test were a solar cell witness plate to characterize how the solar cells would respond to the anode glow, a video camera to determine the

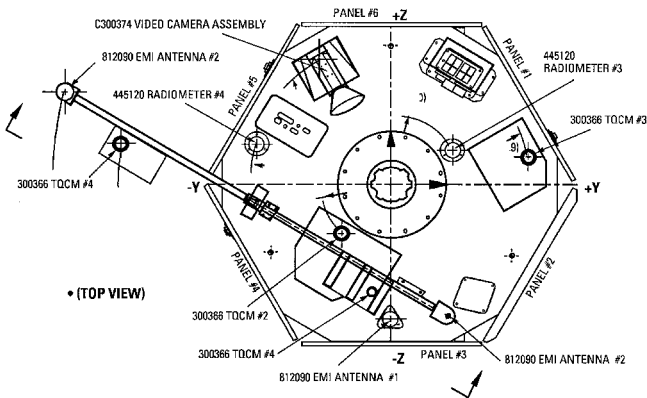


Fig. 7 Diagnostic package device layout.

appropriate shutter speed, a radiometer to characterize how it would perform relative to the radiated heat flux of the arcjet, and radiated and conducted EMI measurements of the arcjet and PCU. This early EMI test was performed because facility limitations precluded actual arcjet firings during the system level EMI testing. The IMS test met all of its test objectives including the support of the TRW diagnostics evaluation testing. The EMI data measured during the IMS test indicated that the radiated and conducted EMI from the arcjet and PCU were within the limits required by the program. The exception to this was the broadband emissions below 0.6 MHz. However, there are no instruments aboard ARGOS that have sensitivities in this frequency range.

Before the integration of ESEK, the flight structure was integrated with mass mockups and successfully completed a structural qualification testing, including measurement of the modal frequencies. After the mockups were removed and the structure passed a posttest inspection, the flight arcjet, power cable, and PCU were integrated with the structure, and the alignment of the thruster was completed. The PFS platform followed, and the propellant line connected to the thruster. The rest of the diagnostics platform equipment was installed followed by the electronics boxes mounted to the side panels, which were subsequently mounted to the core frame. Following hipot testing and thermal vacuum bakeout, interfacing harnesses were integrated, trimmed to length, and completed.

With the integration of the flight unit complete, an initial functional test was performed to check out the interfaces between the

individual subsystems and the CCU. Aliveness tests were also performed, including the monitoring of bus current and voltage as a function of subsystem on/off operation. During the system level integration testing, some interface issues were identified and corrected before entering into phase III of the program in February 1997.

Phase III: Flight Qualification and Delivery

Software Verification

The first test performed on the flight unit in phase III was the flight software acceptance test to verify the ability of the flight software to control the flight unit. This test identified some minor software modifications, as well as one significant interface issue. During the first low-power PCU test with the PCU integrated into the flight unit, it was determined that three signal return lines from the PCU were not connected to chassis ground within the flight harness. A harness adapter was installed, which brought these return lines out from the PCU and grounded them close to the CCU. The PCU was then successfully operated at 4 kW, approximately one year since its last functional test and after two ground transports.

EMC Testing

Following the software verification test, the system EMC test was performed, during which the PCU was operated at full power, 26 kW, for the first time in the fully integrated flight unit. During these tests, the PCU was operated with an arcjet simulator at full power approximately 60 times. For these runs, 80% were 10 min in duration or longer, and the PCU efficiency ranged from 95 to 96%. Input and output current was monitored to verify stability and operation of all three output stages of the PCU. The EMC testing included the full suite of tests identified in MIL-STD-461C and MIL-STD-1540. Susceptibilities were noted during the CS01 and CS02 tests, but nothing that required design or hardware changes.⁷

The PIU was found to be damaged as a result of the CS06 test when, during EMC inrush current testing, current was measured on two of the three heater buses. Although the heaters were disabled, current was still being drawn by the heaters when power was applied to the heater bus. Troubleshooting determined that the transistors for each of the heater circuits were exposed to twice their design rating voltage during EMC testing. Based on the actual spacecraft interface, it was determined that the PIU was overexposed during the CS06 test and that a design change of the board was not required. The PIU was repaired and unit level functional, vibration, and thermal cycle testing was performed before reinstallation into the flight unit. Further inrush current and input surge tests were completed successfully.

During RS03 testing, in the middle of a 26-kW PCU run, the test facility power was momentarily brought down due to a lighting storm. As a result, the flight unit ground support equipment (GSE) power supply was shut down as was the flight unit. A gradual power-up test determined all functions were nominal. It was also determined that, when power was temporarily removed from the flight unit, high power was not removed and then immediately resupplied to the PCU, which could have damaged the unit. Based on this event, an uninterruptible power supply was integrated with the GSE, and the flight software boot-up procedure was revised to protect the PCU from a sudden power-down and power-up event.

Random Vibration Test

The flight unit vibration testing was conducted following the EMC test, and the results are documented in Ref. 8. Before the vibration test, 19 test accelerometers were installed throughout the flight unit, a previbration leak test was performed on the thruster to verify no leakage, and the flight battery and propellant mass simulators were installed.

In each axis, the flight unit was first subjected to a low-level sine sweep to characterize its resonant frequencies, followed by the random vibration test. After each random vibration test, the sine sweep was repeated to determine if any resonant frequencies of

the unit changed. No frequency changes were noted, indicating no changes in the structural integrity of the vehicle.

Following the vibration test, a postvibration functional test was performed on the flight unit. During this test, two hardware problems were found. The first problem was that the videocamera system did not produce a nominal video frame. This problem was initially found during the EMC testing and attributed to contamination found in the video cable. This time, a loose connection was found. The cable was removed and replaced, and the video camera system performed nominally. The resistance of the other pixel clock cables was checked and found to be nominal and x rays determined that no other connectors needed to be replaced.

The second hardware problem was in TQCM 1 sensor located on the diagnostic tower, which measured a significantly lower frequency than expected. The problem was isolated to the sensor itself, which was removed from the spacecraft and returned to the supplier for disassembly, inspection, and rework. The rework involved adding additional potting material to support the flexure of the internal crystal mount. This repair was used on previous TQCMs on other flight programs.

Thermal Vacuum Test

Following the postvibration functional test, the flight unit was prepared for the thermal vacuum test. The EM battery subassemblies were installed, and two ion gauges were temporarily suspended within the flight unit in order to read internal flight unit pressures during the thermal vacuum test. The PCU was connected to the arcjet simulator via special connections through the vacuum chamber walls. Flight and test thermal insulation was installed, and just before thermal vacuum testing, the propellant feed subsystem was pressurized to 1.5×10^4 torr using a 90% GN₂, 10% GHe mixture in preparation for the leak testing to be performed after the thermal vacuum test.

Before installing the EM battery subassemblies, a series of tests were performed to verify the integrity of the battery subassemblies, especially because they had exceeded their activation lifetime by 1 month. Each battery was charged and discharged, and each battery cell was checked to determine its state of health. Although the capacity of the battery subassemblies was lower than when they were first activated (50 A · h vs 70 A · h), there was no indication the battery subassemblies would be unable to support the test. As a precaution, it was decided that the PCU firings would be limited to 10 min during the thermal vacuum test. The EM battery subassemblies were then charged to 50 A · h with an external power supply. The flight battery charger was exercised briefly at the beginning of the charge operation and at the end to verify that the charger did function with the battery subassemblies installed. The internal battery temperatures were monitored during the charging to ensure safe charging temperatures. These temperatures never exceeded 32°C.

While final preparations were underway for the test, a rising temperature was noted on the internal battery thermistor for one battery subassembly. This temperature reached approximately 58°C before decreasing, and a distinct odor was also present in the thermal vacuum chamber. The battery subassembly was promptly removed from the spacecraft, a hole approximately 0.64 cm in diameter was discovered in the battery case, and some contamination of the flight unit was evident.

After the EM battery was removed, its lid was removed, and a black residue was found on the top surface of the battery. A tape test was performed on the interior of the flight unit to determine the extent of contamination within the flight unit. Samples were collected from various locations within the vehicle to determine if any potassium hydroxide electrolyte was released from the battery. All samples taken showed the surfaces to be neutral. Therefore, it was concluded that no electrolyte contamination occurred.

The other major concern was the conductive nature of the particulate contamination, which included copper and carbon. The failed battery was immediately adjacent to the PCU, which controls all of the ESEX high power. Furthermore, the hole in the battery case had direct line of sight to a series of vent holes in the side of the PCU. After the PCU was opened for contamination inspection, it

was determined that a terminal block had been mounted over the PCU vent holes closest to where the battery hole had formed. This terminal block protected the PCU from considerable contamination. Surface resistance measurements taken on the PCU output inductors and inside the battery showed an open circuit. The conclusion from these measurements is that the contamination from the battery was virtually nonconductive.

The root cause of the failure is believed to be a result of exceeding the design life of the battery. The activation life of the battery is 18 months. The EM battery subassemblies were activated 19 months earlier. During this time, dendrites could have formed and caused a short circuit within a cell. In addition, the design specified only 10 charge/discharge cycles, whereas the EM battery subassemblies had been charged 12 times. The probable cause of this failure increased the importance of activating the batteries as close to launch as possible to keep the activation time with specification limits on-orbit.

While the cause of the battery failure was investigated, the spacecraft was cleaned, the remaining two battery subassemblies were removed from the flight unit, and the flight unit was reconfigured to be powered through the vacuum chamber wall using an external power supply.

The thermal vacuum test was to be performed with four cold/hot cycles, and high-power PCU functional tests conducted during two cold-to-hot transitions. However, deviations were taken in response to ion gauge measurements during the first full-power PCU test. This 15 min test was terminated after 3 min when the ion gauges within the flight unit indicated pressures were increasing as the PCU was warming up. The PCU was commanded off when the ion gauges registered 1×10^{-4} torr. It was decided to let the flight unit complete the first hot soak to help drive off more outgassing products while the PCU was not running. The next time the PCU was operated at 26 kW, the pressure within the flight unit did not rise above 5.2×10^{-5} torr, and no further pressure problems were encountered during the test.

After the thermal vacuum test was complete and before the thermal vacuum chamber was brought back to atmospheric pressure, an external leak test of the PFS was performed. A standard leak was introduced into the vacuum chamber and measured by a mass spectrometer within the pumping system. After the chamber stabilized again, a second measurement was taken of the gas being pumped from the chamber. Any helium registered during this measurement would be attributed to a leak of the PFS or background helium. The measured leakage was less than the maximum allowable, 1×10^{-4} scc/s.

After the completion of this test, a PFS algorithm verification test was performed to verify the proper incorporation of the PFS flow control algorithm into the flight software. As an example of one of the two tests performed, the PFS was commanded to control to a flow rate setpoint of 160 mg/s. The operational sequence allows for flow rate stabilization within 2 min, which was demonstrated in this test. Following the PFS algorithm test, the PFS propellant tank was repressurized to approximately 1.5×10^4 torr, and an internal leak test of the dual pressure control valve was successfully performed.

Thruster Alignment Verification

After the flight unit was removed from the thermal vacuum chamber, the flight unit weight and lateral Y and Z c.g. values were determined, and the thruster alignment verification was performed. The alignment was measured via a series of theodolite measurements using an alignment fixture centered on top of the arcjet thruster and eight 45-deg targets placed around the perimeter of this fixture. Horizontal and azimuth readings for theodolite in the X and the Y axis were recorded, and photogrammetry was used to verify the theodolite alignment measurements. The results are provided in Fig. 6.

Preship Activities

In July of 1995, the flight unit was placed in temporary storage for six months, after which it was moved to a clean room integration area for some minor rework and the predelivery functional test. As a part of the poststorage test, two tests of the EMI boom were performed because none had been performed after all the proto-

qualification testing. This testing verified free movement of the boom and functionality of the boom ordnance. After the test, the boom was returned to its stowed configuration and the expended ordnance was replaced. Following the completion of all of the rework, the poststorage/predelivery functional test was performed. As a part of this test, a final high-power test of the PCU was performed. ESEX was delivered to the host vehicle integrator's facility on 6 March 1996.

Lessons Learned

One of the final activities of the program was to generate a lessons learned document, identifying, at all program levels, those things that should be remembered for programs to come. Many of these items were programmatic in nature, but some also addressed how the engineering process could be improved. A subset of the lessons learned is provided here, which can benefit not just high-power electric propulsion programs, but any hardware development program.

Testing

The Arcjet ATTD program was structured to include considerable testing at the unit level, as well as throughout the integration process. Nonetheless, one of the primary lessons learned is the importance of testing as many interfaces as possible to identify all incompatibilities between the different components as early as possible. Identifying incompatibilities early allows the program to implement optimum corrections, as opposed to implementing a correction with limitations (such as when the hardware is no longer accessible or when schedule is more critical). One key example is the inadequate testing of the interface between the battery and the battery charger within the PIU. At the unit level, the battery charger was tested using a battery simulator. Whenever the EM batteries were charged, it was accomplished using a power supply at a higher-than-flight charge rate to conserve schedule time. Only at one time throughout the entire program were the two actually tested together and that was strictly to verify the charger's ability to sense the charge level and shut off the charging process. However, once the hardware was on orbit, and the battery was being charged by the flight charger, instabilities were discovered that produced a very inefficient charging cycle and may have ultimately contributed to the early failure of the flight battery. Had the flight battery charger and the available engineering model battery been integrated and tested through a charge cycle or two, this instability may have been discovered and corrected on the ground. Once the flight hardware was on-orbit, there were very few options for working through this problem.

Team Efforts

ESEX is the culmination of over 10 years of very dedicated effort by numerous contractor and government personnel. The cohesive team efforts of all of these team members maximized the effectiveness and minimized overall cost and schedule of the program due to the prevalence of a can-do attitude. Although many lessons learned occur as a result of negative events, this lesson was learned from many positive events on the ESEX program when the entire team pulled resources together to work a problem. Problems were solved quicker and, hence, cheaper because of the team effort approach. Two examples can be used to illustrate the positive effect of this approach. In the first example, the original arcjet start circuit failed to successfully ignite the arcjet. The Air Force, PAC, and TRW engineers devised and executed a test program at AFRL that defined the correct requirements for this start circuit. These modifications were implemented, and successful starts were observed on every on-orbit firing. The second example is with respect to the assignment of ESEX to ARGOS after PDR. Because the ESEX flight unit design had been baselined before it had been assigned to a host vehicle, there were some interface incompatibilities in the areas of command and telemetry, power, allowable envelope, etc., when the ARGOS spacecraft had been identified as the ESEX host vehicle. All organizations worked to implement the minimum number of changes on both sides of the interface to minimize the overall government cost impact.

Flight Telemetry

A lesson learned from flight operations was that provisions should be made early in any flight program to maximize the amount of on-orbit telemetry available to the flight-operations/experimenter team(s). In the specific case of ESEX, additional telemetry would have permitted the flight experiment team to better determine propellant feed subsystem, arcjet, and battery performance. Ideally, a flight unit should be instrumented on-orbit as it is during ground test to identify clearly the possible modes during on-orbit operations. Obviously this desire must be traded against cost, schedule, and hardware constraints, but the priority of data during operations is clearly the highest, second only to hardware safety.

"Trust Your Gut"

There were times in the program when problems arose and individuals would state, "I thought we might have a problem here." In some cases, the problems arose out of performing engineering tasks and were unavoidable. In other cases, intuition could have prevented problems. For example, the power cable between the PCU and the arcjet had been designed to allow testing of the PCU at full power once it had been integrated into the flight unit. Specifically, a threaded connection allowed a ground-test-only copper adapter to be screwed into it and attached to welding cable. This assembly shunted PCU output power from the PCU to a resistive load that simulated the arcjet. The first time this adapter was to be used, the technician responsible for making the appropriate connections looked at the female threads in the cable and the male threads on the adapter and thought there was potential for galling. This was a particular concern because both sides of the connection were made of copper, a very soft metal prone to galling. However, the mechanic proceeded with screwing the two pieces together, and galling did occur. Considerable effort to disconnect the two pieces failed, and considerable rework was required to correct the configuration for testing and flight. This example is not presented to suggest failure on the part of the technician, but to provide a good representation of the lesson learned. Ideally, what should have happened is that the technician should have "trusted his gut" and highlighted the potential problem to the program test crew before proceeding.

Communication

During the technical development effort, problems or issues occurred as expected in a development program. The amount of communication of the problems to program management directly affected the ultimate impact, both good and bad. In general, the sooner program management (customer and contractor) knew of the problem, the sooner resources were allocated to alleviate the potential problem and to reduce the overall impact. There are several examples (both good and bad) of this phenomenon. One such example happened during system-level testing when an anomaly was observed in the EMI electronics. The test engineers alerted management and a team of experts was compiled to address the issue. Because these personnel collectively had a wealth of engineering expertise, the problem was identified and remedied in a matter of days, avoiding schedule impact at one of the highest visibility points in the program. When communication of anomalies did not occur, it was usually due to a desire to remedy the problem as quickly as possible without involving outside parties. This is, at least in part, due to a natural engineer's tendency to "just fix the problem." This mindset often resulted in a larger overall impact (cost and/or schedule) because the abilities of the full team were not brought to bear.

Monthly Reporting

At program inception, monthly technical reports were required. These reports, proved to be an invaluable resource for a number of reasons. The reports often documented the decision tree for resolution of technical problems, as well as the analyses and trade studies of alternate solutions. This insight often allowed future decisions to be made in the same context, reducing the amount of rework and avoiding decisions that conflicted with each other. As the program schedule stretched out, the reports acted as a continuum of knowledge for the program management, assisting in the transition as technical personnel came and went. Furthermore, when it came time to generate the final report, these reports detailed a chronological history of the program, enabling the final report to be generated for significantly less than it would have cost to task all of the personnel involved.

Summary

The efforts described within this paper summarize the development, fabrication, assembly, and qualification testing of the highest steady-state powered spacecraft flown to date, the ESEX 30-kW arcjet flight experiment. ESEX is the culmination of over 10 years of very dedicated effort by numerous contractor and government personnel to validate high-power electric propulsion on-orbit and verify its compatibility with U.S. Air Force, Department of Defense, and commercial satellites. The true team effort that prevailed throughout the ESEX program was a primary contributor to its success.

Acknowledgments

The author would like to fully acknowledge all of the individuals who supported this program, technically, administratively, or otherwise. Key individuals deserving specific recognition include D. Baxter, J. Beiss, W. Hughes, D. Lee, B. Manly, N. J. Stevens, R. Tobias, and S. Zafran from TRW Space and Electronics Group; R. J. Cassady, W. A. Hoskins, and C. Vaughan from General Dynamics Corporation; H. Clevinger, W. Johnson, and R. Ruble from Orbital Sciences Corporation; D. Bromaghim and A. Sutton from the U.S. Air Force Research Laboratory; and L. Johnson from the Jet Propulsion Laboratory.

References

- ¹Pollard, J. E., Marvin, D. C., Janson, S. W., Jackson, D. E., and Jenkin, A. B., "Electric Propulsion Flight Experience and Technology Readiness," AIAA Paper 93-2221, June 1993.
- ²Pencil, E. J., Sarmiento, C. J., Lichtin, D. A., Palchefskey, J. W., and Bororad, A. L., "Low Power Arcjet System Spacecraft Impacts," AIAA Paper 93-2392, June 1993.
- ³Zafran, S., "Arcjet Hydrazine Propulsion System Integration Testing," International Electric Propulsion Conf., IEPC Paper 91-013, Oct. 1991.
- ⁴Lichon, P. J., and Cassady, R. J., "Endurance Test of an Improved Performance 30 Kilowatt Class Arcjet Thruster," AIAA Paper 90-2533, July 1990.
- ⁵Bromaghim, D. R., LeDuc, J. R., Salasovich, R. M., Spanjers, G. G., Fife, J. M., Dulligan, M. J., Schilling, J. H., White, D. C., and Johnson, L. K., "Review of the Electric Propulsion Space Experiment (ESEX) Program," *Journal of Propulsion and Power*, Vol. 18, No. 4, 2002, pp. 723-730.
- ⁶Cassady, R. J., Hoskins, W. A., and Vaughan, C. E., "Development and Flight Qualification of a 26-Kilowatt Arcjet Propulsion Subsystem," *Journal of Propulsion and Power*, Vol. 18, No. 4, 2002, pp. 740-748.
- ⁷Mendell, W. D., "Electric Propulsion Space Experiment (ESEX) EMC Test Report," TRW Space and Electronics Group, TRW Document 95.M541.4-035, Redondo Beach, CA, June 1995.
- ⁸Barone, T. J., "Arcjet Payload Protoflight Test Report," TRW Space and Electronics Group, TRW Document M533.5.95-071, Redondo Beach, CA, May 1995.